^{19}F NMR Studies of Plasminogen Activator Inhibitor-1†

Glenn L. Abbott,[‡,⊥] Grant E. Blouse,[§,+] Michel J. Perron,[§,+] Joseph D. Shore,[§,+] Linda A. Luck,[||] and Arthur G. Szabo*[,⊥]

Department of Chemistry, University of Waterloo, 200 University Avenue West, Waterloo, Ontario N2L 3G1, Canada, Division of Biochemical Research, Henry Ford Health Sciences Center, One Ford Place 5-D, Detroit, Michigan 48202, Department of Pharmacology, Wayne State University School of Medicine, 540 East Canfield Drive, Detroit, Michigan 48201, Department of Chemistry, Clarkson University, Potsdam, New York, New York 13699, and Department of Chemistry, Wilfrid Laurier University, 75 University Avenue West, Waterloo, Ontario N2L 3C5, Canada

Received September 8, 2003; Revised Manuscript Received December 19, 2003

ABSTRACT: Plasminogen activator inhibitor-1 (PAI-1) is a 43 kDa protein involved in the regulation of fibrinolysis. PAI-1 is the principal inhibitor of tissue-type plasminogen activator (t-PA), trapping the proteinase as an acyl-enzyme covalent complex (∼105 kDa). Four single tryptophan mutants of PAI-1 have been constructed in which three of the four tryptophan residues (Trp86, Trp139, Trp175, and Trp262) were replaced with phenylalanine. Biosynthetic incorporation of 5-fluorotryptophan (5F-Trp) into wild-type PAI-1 (5FW wtPAI-1) and the single tryptophan mutants (5FW86, 5FW139, 5FW175, and 5FW262) was achieved, allowing a ^{19}F NMR spectroscopic study of PAI-1 in its active and cleaved forms and in complex with t-PA. The ^{19}F NMR spectrum of active 5FW wtPAI-1 shows four clearly resolved peaks at −39.20, −49.26, −50.74, and −52.57 ppm relative to trifluoroacetic acid at 0 ppm. Unequivocal assignments of these four resonances in the spectrum of 5FW wtPAI-1 to specific tryptophan residues were accomplished by measuring the chemical shifts of the ^{19}F resonances of the single tryptophan mutants. There was close agreement between the resonances observed in 5FW wtPAI-1 and of those in the mutants for all three protein forms. This would imply little structural perturbation in the local structures of the tryptophan residues resulting from substitution by phenylalanine. The 5FW wtPAI-1 was observed to have lower second-order rate constant (k_{app}) for the inhibition of t-PA than the natural tryptophan wtPAI-1, suggesting that the decreased activity may result from a small structural effect of the fluorine substituent of the indole ring. Further alterations in the k_{app} and the stoichiometry of inhibition (SI) were observed in each of the mutants indicating an effect of the three tryptophan to phenylalanine mutations. Detailed interpretation of the ^{19}F NMR spectra of the PAI-1 mutants provides insights into the local segmental structure of the active form of the proteins and the structural changes that occur in the cleaved and t-PA complexed forms.

Serpins[1] (serine proteinase inhibitors) are a large superfamily of proteins that are intimately involved in a diverse range of physiological processes such as blood coagulation, fibrinolysis, complement activation, inflammation, and matrix remodeling (*1*−*5*). Many serpins inhibit the serine proteinases of the chymotrypsin family and represent about 10% of the total protein in vertebrate plasma (*1*−*5*). Serpins have also been identified that cross-react with cysteine proteinases (*6*) and have been recently found in prokaryotes (*7*). In addition, serpins have been identified with no inhibitory function at all and are involved in roles such as blood pressure regulation, hormone transport, and chaperones (*1*−*5*). Serpins range from 350 to 500 amino acids in length and share a highly conserved tertiary structure consisting of three β-sheets (A−C), seven to nine α-helices (A−I), and a solvent-exposed reactive center loop (RCL) that includes residues P16−P10′ (*2*, *4*, *8*). Schechter and Berger developed

† This work was supported by the Heart and Stroke Foundation of Ontario. L.A.L. acknowledges partial funding for this work from the Petroleum Research Fund (Grant 36825-AC4).

* To whom correspondence should be addressed: Arthur G. Szabo, Ph.D., Office of the Dean of Science, Rm. N1048, Science Bldg., Wilfrid Laurier University, 75 University Avenue West, Waterloo, Ontario N2L 3C5, Canada. Telephone: 1-519-884-0710 x-2129. Fax: 1-519-884-0464. E-mail: aszabo@wlu.ca.

‡ University of Waterloo.

§ Henry Ford Health Sciences Center.

+ Wayne State University School of Medicine.

|| Clarkson University.

⊥ Wilfrid Laurier University.

[1] Abbreviations: Serpin, serine proteinase inhibitor; PAI-1, plasminogen activator inhibitor-1; t-PA, tissue-type plasminogen activator; RCL, reactive center loop; P1−P1′ and P16−P10′, identify specific amino acid residues located within the RCL according to the nomenclature set forth by Schechter and Berger; 5F-Trp, 5-fluorotryptophan; 7A-Trp, 7-azatryptophan; 5FW wtPAI-1, 5F-Trp-incorporated wild-type PAI-1; 5FW86, 5FW139, 5FW175, and 5FW262 refer to the single tryptophan mutants of PAI-1 in which three of the four tryptophan residues were mutated to phenylalanine residues and the remaining tryptophan residue was biosynthetically replaced with 5F-Trp and denoted as such; ^{19}F NMR, fluorine nuclear magnetic resonance; IPTG, isopropyl-β-D-thiogalactopyranoside; Hepes, 4-(2-hydroxyethyl) piperazine-1-ethane sulfonic acid; k_{app}, apparent second-order rate constant of proteinase inhibition; SI, stoichiometry of inhibition; TFA, trifluoroacetic acid; SDS−PAGE, sodium dodecyl sulfate−polyacrylamide gel electrophoresis; EACA, ϵ-aminocaproic acid; EDTA, ethylenediaminetetraaccetic acid; HPLC, high-pressure liquid chromatography; MES, mercaptoethanesulfonic acid; MS, mass spectrometry; GGR, glucose−galactose sugar binding protein; LBP, leucine-specific protein; TROSY, transverse relaxation-optimized spectroscopy.

10.1021/bi035618a CCC: $27.50
Published on Web 01/24/2004

a system of nomenclature to describe specific residues within the RCL (*9*). In this nomenclature, P16 through P1 denote those residues on the amino-terminal side of the scissile bond, while those designated as P1′ to P10′ reside on the carboxy-terminal side of the scissile bond. The P1−P1′ residues contained within the RCL mimic the ideal proteinase substrate and thus serve as the "bait" peptide for a serpin's target proteinase. Cleavage of the P1−P1′ scissile bond by the target proteinase permits insertion of the RCL into the central β-sheet A as strand s4A (*10*). This extensive conformational change, known as the "stressed to relaxed" transition (*11*), allows the serpin to achieve an increased stability, yielding a serpin−proteinase pair that is kinetically trapped as an acyl-enzyme covalent complex (*12*, *13*). Stabilization of the complex is achieved by the refolding of the cleaved inhibitor in which the covalently bound proteinase is translocated to the distal end of the serpin via insertion of the RCL into β-sheet A (*14*−*16*). The separation of the P1−P1′ residues by approximately 70 Å, as well as distortion of the proteinase structure, ensures that deacylation is irreversible (*13*, *17*−*20*). Thus, serpins are referred to as "suicide substrates" (*4*).

Plasminogen activator inhibitor-1 (PAI-1) is a serpin found in plasma, platelets, endothelial cells, fibrosarcoma cells, and hepatoma cells (*21*). The vascular endothelial cells are believed to be the primary site of synthesis for plasma PAI-1 (*22*). PAI-1 is the principal inhibitor of tissue-type plasminogen activator (t-PA) and urokinase-type plasminogen activator (u-PA) (*23*). PAI-1 shares the same highly ordered tertiary structure with other serpins described previously and has been expressed as 43 kDa protein in *Escherichia coli* (*24*). PAI-1 is unique because it is the only member among the serpin superfamily known to spontaneously adopt a latent conformation in which the N-terminal portion of the RCL is inserted into β-sheet A without cleavage of the P1−P1′ residues (*25*). Crystal structures have been determined for the active (*26*, *27*), cleaved (*28*), and latent forms (*25*) of PAI-1. These structures have provided limited information on the role of conformational change that is the basis of the serpin inhibitory mechanism. Recently, the first X-ray crystal structure of a serpin−proteinase pair, trypsin−α_1-antitrypsin, was solved (*13*). This crystal structure provides only a static picture of the complex and offers little information on dynamics and conformational heterogeneity. Optical studies by circular dichroism and intrinsic fluorescence (*29*−*34*) have yielded solution-state information on conformational changes that occur in PAI-1 upon cleavage or latency. However, fluorescence techniques cannot be extended to investigation of PAI-1 in complex with its target proteinase, because the observed fluorescence would be an average signal of the combined tryptophans from both protein partners.

PAI-1 contains four tryptophan residues located at positions 86, 139, 175, and 262 (Figure 1). These residues are found in different structural segments and thus distinct environments of the protein. Trp86 is located at the top of helix D on a turn leading into sheet 2A, Trp139 is located on helix F, Trp175 is located at the very top of sheet 3A in the conserved breach region, and Trp262 is found on helix H. The fluorescence of each tryptophan residue is potentially capable of reporting on its local environment and of any changes in this environment due segmental or domain

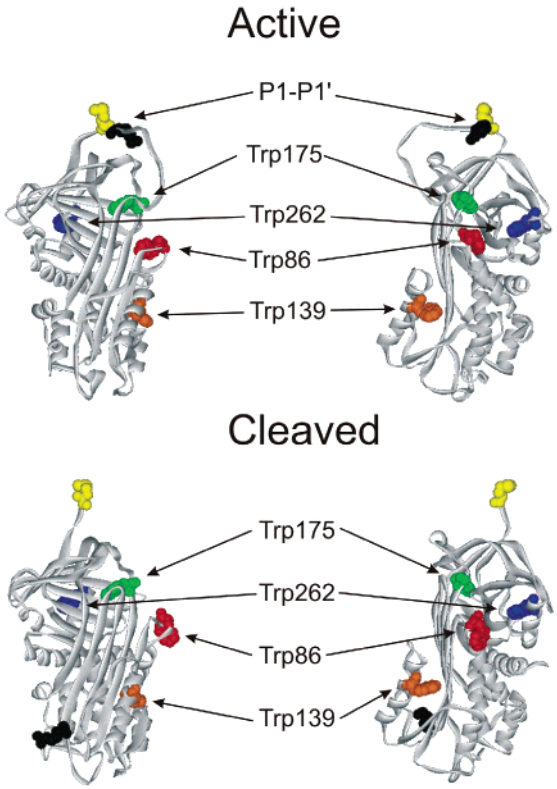

FIGURE 1: The X-ray crystal structures of the active (PDB 1B3K, chain A) (*26*) and cleaved (PDB 9PAI-1) (*28*) conformations of PAI-1. Structures on the left side are an orthogonal view with respect to the structures viewed on the right side. These two profiles are shown for both the active (top) and cleaved conformations (bottom) indicating the location and position of each of the tryptophan residues. Tryptophan residues are shown as space filling (CPK) representations. Trp86 is red, Trp139 is orange, Trp175 is green, and Trp262 is blue. The P1−P1′ residues of the RCL are shown as yellow (Met346) and black (Arg347). Structures were generated in ViewerLite 5.0 (Accelrys, San Diego, CA).

movements. The biosynthetic incorporation of tryptophan analogues would permit the study of conformational change of PAI-1 in the presence of other proteins. A recent study demonstrated a concerted structural transition in the PAI-1 inhibition mechanism with PAI-1 labeled at all four positions with the tryptophan analogue 7-azatryptophan (7A-Trp) (*24*). In addition to their unique fluorescence properties, the fluorinated tryptophan analogues 4-fluorotryptophan, 5-fluorotryptophan, and 6-fluorotryptophan would allow ^{19}F NMR studies of proteins and of their interactions with other proteins (*35*, *36*).

NMR methods can be a powerful tool for the characterization of protein structure and function (*37*). When specific residues in a protein can be assigned to resonances in the NMR spectrum, one can probe structure and dynamics of both the protein and its complexes. Early 1D NMR experiments of serpins proved to be inadequate owing to poor resolution (*38*−*43*). 2D NMR studies have provided a picture of global structural changes occurring in the serpin in the noncovalent Michaelis complex and in the cleaved serpin (*44*) and an incomplete three-dimensional structural determination of the serpin in the covalent complex (*20*). Assigning all the resonances to specific amino acid residues in the serpin−proteinase pair is a difficult and formidable challenge in a complex this large. With higher fields, multidimensional experiments, and advanced pulse sequences

such as TROSY, proteins of high molecular weights have been studied (*45*, *46*). Even with these sophisticated methods, there are many proteins and complexes that are not amenable to study. The PAI-1 system is one that does not show promise for full structural analysis by NMR; thus, we have resorted to another method to obtain information from this protein and its complexes. ^{19}F NMR provides few obstacles in assigning resonances to specific chemical groups and lower cost in sample preparation while still providing information on structure and dynamics. The ^{19}F nucleus is 100% abundant and has a sensitivity that is comparable to that of ^{1}H with no background signals. The ^{19}F NMR chemical shifts extend over a larger range than ^{1}H chemical shifts, and the experiments can be performed in one dimension due to the less complex nature of the resonances. The fluorine nucleus is highly sensitive to its environment due to the lone pairs of electrons, which provides a useful probe for determining conformational change in a specific area of a protein. Small changes in local environment can be assessed by this method. The fluorine nucleus can be biosynthetically incorporated into proteins by routine methods and many of the fluorinated amino acids are commercially available (*35*, *47*, *48*).

To date, few NMR studies have focused on serpins in complex with their target proteinases (*17*, *20*, *41*, *44*) with one ^{19}F NMR study on the serpin antithrombin III and of its interaction with heparin (*49*). The utility of ^{19}F NMR in investigating proteins and nucleic acids and their interactions with their ligands, receptors, and inhibitors is extensive (*35*, *36*). ^{19}F NMR studies on serpins may provide new information on conformational changes around specific residues in their native, complexed, and cleaved forms.

In this paper, we report the successful incorporation of the tryptophan analogue 5F-Trp into wtPAI-1 and its single tryptophan mutants allowing assignment of the individual ^{19}F NMR resonances for each of the tryptophan residues. 5F-Trp was chosen over other fluorinated amino acid derivatives due to its availability, cost, and wider dispersion of chemical shifts with different environments as observed for glucose−galactose sugar binding protein (GGR) (*50*) and leucine-specific protein (LBP) (*51*). ^{19}F NMR experiments were performed on the active and cleaved forms of PAI-1 and of PAI-1 in complex with t-PA. It was shown that significant structural changes occurred in the local environments surrounding Trp86 and Trp139 and to a lesser extent in Trp175 and Trp262 in PAI-1 upon interaction with t-PA (i.e., complexed), in its cleaved conformation, or both.

MATERIALS AND METHODS

Materials. L-Tryptophan, 5-fluoro-DL-tryptophan, chloramphenicol, kanamycin, ampicillin, DNase I, RNase A, phenylmethylsulfonyl fluoride (PMSF), ethylenediaminetetraacetic acid disodium salt (EDTA), 2-[4-(2-hydroxyethyl)-1-piperazine] ethanesulfonic acid (Hepes), glycerol, magnesium sulfate, calcium chloride, vitamin B1 (thiamine), sodium phosphate dibasic heptahydrate, sodium phosphate monobasic monohydrate, potassium phosphate monobasic, ammonium chloride, ammonium sulfate, sodium hydroxide, potassium hydroxide, 2-amino-2-(hydroxymethyl)-1,3-propanediol (Tris), triethylamine (TEA), hydrochloric acid, ammonium hydroxide, and sodium chloride were purchased from Sigma (St. Louis, MO) or VWR (EM Science, Mississauga, Canada). Trypticase peptone, yeast extract, and CASamino acids were purchased from either Becton, Dickinson and Co. (Sparks, MD) or Difco (Detroit, MI). Isopropyl-β-D-thiogalactopyranoside (IPTG) was purchased from Melford Labs (Suffolk, U.K.). Spectrozyme^{t-PA} (CH_3SO_2-D-HHT-Gly-Arg-*p*NA) was obtained from American Diagnostica Inc. (Greenwich, CT). All kinetic measurements were performed at pH 7.4 in 30 mM Hepes, 135 mM NaCl, 1 mM EDTA, and 0.1% PEG 8000 in acrylic sample cuvettes coated with 0.1% PEG 20 000 for the reduction of protein adsorption. Heparin, phenyl, and SP-substituted Sepharose were purchased from Amersham Biosciences (Uppsala, Sweden). HPLC/spectrophotometric grade sodium acetate-trihydrate, glacial acetic acid, and methanol were obtained from J. T. Baker (Phillipsburg, NJ). 3 N mercaptoethanesulfonic acid (MES) was purchased from Pierce (Rockford, IL). Sodium dodecyl sulfate and acrylamide were obtained from BioRad (Hercules, CA).

Table 1: Mutagenic Oligonucleotides

mutation	oligonucleotide primer sequences[a]
W86F	5′$_{342}$-dGATCTCATCCTTGTT*A*A*A*TGGCCCCATGAGCT-3′$_{311}$
W139F	5′$_{501}$-dTGTGTGTGTCTTCAC*A*A*A*GTCATTGATGATGA-3′$_{470}$
W175F	5′$_{609}$-dGGGGAAGGGAGTCTT*G*AACTGGCCGTTGAAGT-3′$_{578}$
W262F	5′$_{609}$-dGGTCATGTTGCCTTT*G*AAGTGGCTGATGAGCT-3′$_{578}$

[a] The numbering for oligonucleotide 5′ and 3′ designations is labeled according to the sequence of the human PAI-1 gene without the signal peptide. Substituted bases are indicated by the italic nucleotides.

Recombinant PAI-1 Mutagenesis, Expression, and Purification. The preparation of recombinant human PAI-1 in the pET-24d vector (Novagen) has been previously described (*24*). For some mutants, the PAI-1 gene was transferred into pET-24c vector (Novagen) to help improve mutagenesis efficiency. The W86F, W139F, W175F, and W262F mutations or combinations thereof were engineered by site-directed mutagenesis using the Muta-Gene Phagmid In Vitro Mutagenesis kit (Bio-Rad) and the method of Kunkel (*52*, *53*). The mutagenic oligonucleotides listed in Table 1 were used to generate the individual W86F, W139F, W175F, and W262F mutations in the PAI-1 gene. For the preparation of the multiple tryptophan to phenylalanine mutations, multiple primers were included in the mutagenesis reaction using a wtPAI-1 background (Trp86, Trp139, and Trp175) or a W175F + W262F background template (Trp262). All mutations were confirmed by DNA sequencing of the full length PAI-1 gene. For recombinant expression in *E. coli*, the wtPAI-1 construct was transformed into the host BL21(DE3) pLysS (Novagen) and cultured in LB media to an OD_{600} of 0.3−0.5 prior to induction of protein expression for 2−3 h by the addition of IPTG to a final concentration of 1 mM at 30 °C. Bacterial lysates were obtained by sonication. The soluble active and latent PAI-1 fractions were purified and separated by heparin, phenyl, and SP-substituted Sepharose chromatography as previously described (*24*). Further purification of active PAI-1 from the latent fraction was performed using β-anhydrotrypsin coupled to a 1 mL NHS-activated HiTrap (Amersham Biosciences) column following manufacturers guidelines (*54*). Preparation of β-anhydrotrypsin has been described previously (*55*). Biosynthetic incorporation of 5F-Trp into PAI-1 required the use of an auxotrophic strain of *E. coli*, W3110*TrpA88*(DE3). The host strain was further modified by the introduction of

the pLysS plasmid (Novagen) containing the gene for T7 lysozyme, a repressor to the T7 promoter, to reduce background expression prior to analogue supplementation. The method for incorporation of 5F-Trp as described by Hogue et al. (*47*) was used with the following modifications. Briefly, host cells containing PAI-1 pET-24d constructs are cultured in M9 minimal media (*56*) supplemented per liter with 2% CASamino acids, 0.01% thiamin, 2 mM $MgSO_4$, 0.4% glucose, 0.4% glycerol, 0.1 mM $CaCl_2$, and 0.02 mM L-tryptophan. Cells reached a limiting density after ~16 h of incubation at 37 °C and consumption of all available L-tryptophan ($OD_{600} \approx 0.8-1.0$), after which DL-5F-Trp was added to a final concentration of 0.5 mM. Following a 10-min incubation in the presence of 5F-Trp, protein expression was induced by IPTG for 2−3 h, cell lysates were harvested, and PAI-1 protein was purified as previously mentioned. Bacterial cultures were cooled in an ice bath 15 min postinduction and maintained at 30 °C. 5F-Trp labeled proteins were dialyzed into 5 mM sodium phosphate, 345 mM NaCl, 1 mM EDTA, and pH 6.6, concentrated on an Amicon stir cell (Amicon Inc., Beverly, MA), snap frozen in liquid nitrogen, and stored at −80 °C. PAI-1 protein concentrations were determined by the Bradford dye-binding assay (*57*) using purified wtPAI-1 as a standard with an extinction coefficient (ϵ_{280}) of 0.93 mL mg^{-1} cm^{-1} and a M_r of 43 000 (*58*, *59*).

Preparation of Cleaved PAI-1. Five milligrams of porcine elastase (Sigma) was coupled to a 1 mL NHS-activated HiTrap column (Amersham Biosciences) following manufacturers guidelines. Elastase cleaves PAI-1 at the P3−P4 peptide bond of the RCL permitting loop insertion without formation of the covalent acyl-enzyme complex (*60*). Subsequently, 5−7 mg of purified active fluorinated PAI-1 protein was fluxed through the elastase column for 30−45 min, after which the column was washed extensively with buffer and the effluent was collected. To ensure complete cleavage, a small aliquot was removed, mixed with t-PA, and run on a 10% SDS−PAGE with appropriate controls. Cleaved proteins were precipitated overnight against solid ammonium sulfate at 4 °C using 12 000−14 000 MWCO dialysis tubing (Spectra-Por, VWR, Mississauga, ON, Canada). Precipitated proteins were resuspended in 5 mM sodium phosphate buffer, 345 mM NaCl, 1 mM EDTA, pH 6.6, snap frozen, and stored at −80 °C.

Preparation of Two-Chain t-PA. Human recombinant t-PA (Activase) was kindly provided by Genentech Inc. (San Francisco, CA). Single-chain t-PA was converted to two-chain t-PA by fluxing through a 1 mL plasmin column (Molecular Innovations, Southfield, MI) and has been described previously (*61*). t-PA was stored at −80 °C in 30 mM sodium phosphate, 135 mM NaCl, 20 mM EACA, 1 mM EDTA, pH 6.6. The concentration of t-PA was determined using the absorptivity coefficient of 1.9 mL mg^{-1} cm^{-1} and the M_r of 63 500. Prior to use, t-PA was thawed at 37 °C for 5 min to dissolve protein aggregates.

Determination of the Level of Tryptophan Analogue Incorporation. Assessment of tryptophan analogue incorporation efficiency was determined by acid hydrolysis of proteins and reverse-phase HPLC developed specifically to quantitate the level of incorporation of tryptophan analogues biosynthetically incorporated into proteins (*62*) (unpublished). Protein hydrolysis was accomplished using 3 N mercaptoethanesulfonic acid (MES) (*63*). An approximately 150 μL aliquot of protein (0.1−0.5 mg) was placed into a 6 mm × 50 mm Pyrex tube (VWR) to which 50 μL of 3 N MES was added. This tube was placed into a larger thick walled glass vacuum vessel and sealed with a threaded Teflon cap housing a two-way valve. The vessel was then subjected to repeated vacuum and purge cycles using ultrahigh purity nitrogen. Hydrolysis was then carried out in either a Waters Workstation (Milford, MA) or a Pierce Reacti-Therm Heating Module (Rockford, IL) that was modified by employing a custom-made aluminum block that held the thick walled vacuum vessel. The vessel and its contents were incubated at 110 °C for 22 h, after which the vessel was removed from the heating module and allowed to cool to room temperature. A 50 μL aliquot of 3 N NaOH was then added to neutralize the acidic contents and the reaction contents were mixed well and briefly centrifuged on a tabletop microfuge. Sample(s) were then dried in a Labconco Centrivap Concentrator (Labconco Corp., Kansas City, MO). The dried hydrolysate was then redissolved in 150 μL of Milli-Q water, gently vortexed, and centrifuged.

Analytical RP-HPLC was accomplished using a Gilson modular design HPLC (Middleton, WI) consisting of two pumps, a manometric module, a dynamic mixer, and a UV detector set at 280 nm. A Rheodyne 7125 injection valve (Cotati, CA) was used equipped with a 50 μL loop. A C-18 reverse-phase analytical column by Alltech (Prevail, 250 mm × 4.6 mm, 5μ) in conjunction with a Zorbax ODS guard column (Hewlett-Packard, Palo Alto, CA) was employed. The outlet tubing was fitted with a back-pressure regulator (Upchurch Scientific, Oak Harbor, WA) rated at 75 psi. This HPLC was interfaced to a desktop computer communicated through a controller. The elution conditions and the gradient employed were modified from those of Delhaye and Landry (*64*) using a 21 min linear gradient from solvent A (70 mM sodium acetate, 5% methanol, 0.025% triethylamine, pH 4.5) to solvent B (100% methanol) at 1 mL/min. The concentrations of tryptophan and 5F-Trp in the hydrolysate were determined using standard additions of tryptophan and 5F-Trp. Twenty microliter injections were performed in duplicate and the averaged integrated absorbances at 280 nm of the tryptophan and 5F-Trp elution peaks were plotted against the concentrations of the standard added and then fit by linear regression. The generated regression equation-(s) were then used to determine the relative amounts of tryptophan and 5F-Trp using the integrated absorbance at 280 nm and the amount of the standard addition added to the sample. To confirm that there was no differential degradation of tryptophan relative to 5F-Trp by the MES hydrolysis conditions, stock solutions were made of the free amino acids tryptophan and 5F-Trp (~180 μM), in which various ratios of the free amino acid solutions were mixed together and then injected. Subsequently, these same stock solutions were then subjected to the identical hydrolysis conditions employed for protein hydrolysis and injected. The integrated peak areas for the treated and untreated samples indicated the recovery of tryptophan ($n = 14$) and 5F-Trp ($n = 5$) was 94.5% ± 2.7% for and 95.4% ± 0.9%, respectively as shown by RP-HPLC analysis.

Effective Inhibitor Concentration. The stoichiometry of inhibition (SI) is defined as the number of moles of inhibitor (serpin) required to inhibit 1 mol of proteinase and has been

described previously (*5*, *24*). Briefly, 200 nM t-PA was preincubated with 0−2-fold concentrations of wtPAI-1 or 5F-Trp-incorporated proteins in a 100 μL volume of 30 mM Hepes, 135 mM NaCl, 1 mM EDTA, 0.1% PEG 8000, pH 7.4, for 60 min at 25 °C. Subsequently, 0.9 mL of 0.1 mM Spectrozyme^{t-PA} chromogenic substrate was added to the reaction mixture, and the initial reaction rates were monitored by the absorbance change at 405 nm using a Varian Cary UV50 UVVIS spectrophotometer. Plotting residual t-PA activity versus molar ratio of PAI-1/t-PA permitted the calculation of the SI by extrapolating the best-fit linear regression of the data to the *x*-intercept. SI determinations were performed in duplicate, repeated, and reported as the mean ± standard deviation.

Apparent Bimolecular Rate Constants for the Binding of 5FW PAI-1 to t-PA. The competitive kinetic method (*65*) was used to determine the apparent second-order rate constants (k_{app}) for the irreversible inhibition of t-PA by wtPAI-1 and 5F-Trp-incorporated proteins using 0.5 mM Spectrozyme^{t-PA}. The procedure has been described elsewhere (*24*, *61*) and performed under pseudo-first-order conditions using 10 nM wtPAI-1, 10−50 nM fluorinated PAI-1 proteins, and 2 nM t-PA. Inhibition progress curves were monitored by the absorbance change at 405 nm using a Varian Cary UV50 UVVIS spectrophotometer and were fit by a single-exponential function with a linear component to obtain the pseudo-first-order rate constant, k_{obs}. The second-order bimolecular rate constant (k_{app}) was obtained by dividing k_{obs} by the functional inhibitor concentration (i.e., inhibitor concentration divided by the SI) and then multiplying by the factor $1 + [S_0]/K_M$ to correct for the competitive effect of the substrate in the serpin−proteinase reaction. The K_M value for t-PA/Spectrozyme^{t-PA} pair was determined by standard Michaelis−Menton kinetic analysis (data not shown) and found to be 77.9 μM. Experiments were performed in triplicate, and data are reported as the mean ± standard deviation.

^{19}F NMR Measurements. ^{19}F NMR spectra were obtained at 564 Hz on a Bruker 600 NMR spectrometer equipped with a 5 mm ^{1}H/^{19}F probe. PAI-1 samples were typically 50−80 μM in 5 mM sodium phosphate, 345 mM NaCl, 1 mM EDTA, and pH 6.6. D_2O (10% (v/v); Cambridge Isotopes, Andover, MA) was added to all samples as the lock solvent. For the t-PA addition experiments, a stoichiometric amount of t-PA was added to PAI-1 proteins and gently mixed by aspiration. The spectrometer was calibrated with 200 μM 5F-Trp to −49.6 ppm relative to trifluoroacetic acid (TFA) at 0 ppm. Standard spectral parameters were 12 000-Hz spectral width, 60° pulse width, 500 ms relaxation delay, temperature at 20 °C with no decoupling. Processing was done with a 25−50 Hz line broadening. To confirm the reproducibility of ^{19}F resonances, protein samples were run at least in triplicate ($n \geq 3$) for both the active forms and in complex with t-PA and in duplicate ($n = 2$) for the cleaved forms. ^{19}F resonances showed ≤0.1 ppm difference between corresponding spectra.

RESULTS

Efficiency of 5F-Trp Incorporation into PAI-1 and its Effect on PAI-1 Expression and Function. The 5F-Trp-incorporated proteins expressed at lower levels than the natural tryptophan containing proteins. Yields were typically 0.67−1.25 mg/L of culture for the fluorinated proteins and 1.25−1.67 mg/L of culture for the natural tryptophan containing wild-type protein. 5FW86 expressed poorly and failed to show production in some instances, whereas the mutant 5FW175 consistently expressed at higher levels than the other fluorinated single tryptophan mutants and was comparable to that of wtPAI-1.

Table 2: The Level of 5F-Trp Incorporation in PAI-1 and PAI-1 Mutants[a]

	level of incorporation (%)
5FW wt	78.9 ± 5.1
5FW86	42.4 ± 2.3
5FW139	80.6 ± 8.0
5FW175	75.5 ± 0.9
5FW262	77.7 ± 1.8

[a] Incorporation efficiency was determined by sulfonic acid hydrolysis of 5F-Trp-containing proteins. Standard additions of L-tryptophan and 5F-DL-Trp to the hydrolysate were performed, and separation and quantitation were performed using RP-HPLC. Results are reported as the percentile ± standard deviation.

Table 3: Kinetic Parameters for wtPAI-1 and 5F-Trp-Labeled PAI-1s[a]

	k_{app} ($\times 10^7$ M^{-1} s^{-1})	SI
wt	1.17 ± 0.33	1.08 ± 0.09
5FW wt	0.61 ± 0.07	1.02 ± 0.03
5FW86	0.16 ± 0.04	1.39 ± 0.24
5FW139	0.16 ± 0.01	1.64 ± 0.20
5FW175	0.46 ± 0.05	1.07 ± 0.02
5FW262	0.58 ± 0.01	2.20 ± 0.04

[a] Kinetic data was acquired from samples measured in 30 mM Hepes, 0.135 mM NaCl, 1 mM EDTA, 0.1% PEG 8000, pH 7.4, and 25 °C. The k_{app} data are reported of the averages of three independent experiments ± standard deviation. SI experiments were performed in duplicate, repeated, and reported as the mean ± standard deviation.

Sulfonic acid hydrolysis of 5F-Trp containing PAI-1s followed by standard addition of known amounts of L-tryptophan and 5F-Trp to the hydrolysates with the subsequent separation and quantitation by analytical RP-HPLC was performed. The levels of 5F-Trp incorporation in PAI-1 mutants are summarized in Table 2. Attempts to use mass spectrometry (MS) to determine the level of incorporation of 5F-Trp in PAI-1 proved to be impractical because the protein precipitated during dialysis into buffers required for MS analysis. The level of expression of 5FW86 was less than the other 5F-Trp containing proteins. The natural tryptophan mutant W86 expressed at levels comparable to the wt protein. Taken together with the low level of incorporation of 5F-Trp in this mutant, this may suggest that the 5F-Trp containing protein does not fold efficiently. The apparent bimolecular rate constant (k_{app}) for the inhibition of t-PA and the stoichiometric index (SI) of the PAI-1 mutants are summarized in Table 3. All mutants retained their inhibitory activity toward t-PA. Where low levels of 5F-Trp incorporation were indicated (e.g., 5FW86), these kinetic data are the weighted average of the fluorinated tryptophan and the natural tryptophan containing proteins.

^{19}F NMR Spectra of 5F-Trp-Incorporated Active PAI-1 Mutants. Figure 2 presents the ^{19}F NMR spectra of 5F-Trp-labeled PAI-1s in their active conformation. Data acquisition typically took 12 h. To check that the PAI-1 mutants

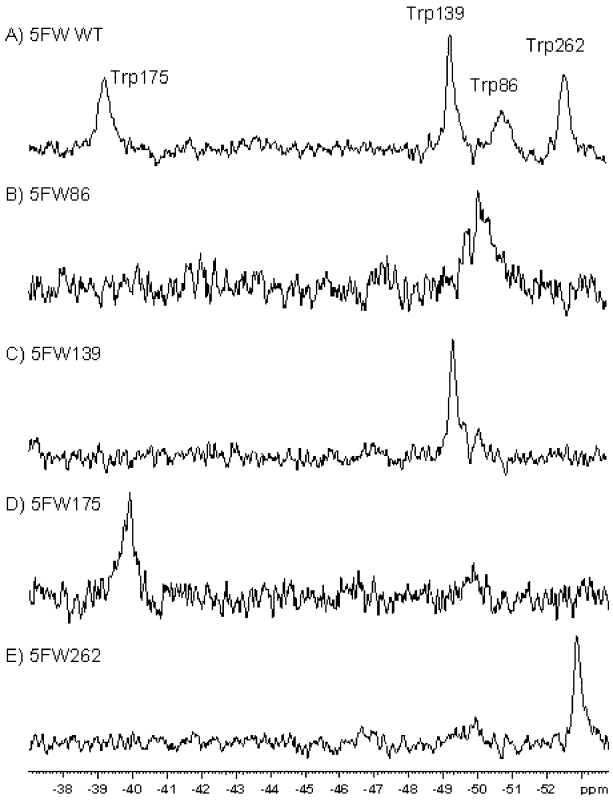

FIGURE 2: The ^{19}F NMR spectra of PAI-1s in the active conformation. 5F-Trp-labeled PAI-1 was typically 50−80 μM in 5 mM sodium phosphate, 345 mM NaCl, 1 mM EDTA, and pH 6.6: (A) 5FW wt, (B) 5FW86, (C) 5FW139, (D) 5FW175, and (E) 5FW262. All samples contained 10% D_2O as the lock solvent. Spectra were acquired at 20 °C at 564 MHz on a Bruker 600 MHz spectrometer. Standard spectral parameters were 12 000-Hz spectral width, 60° pulse width, 500 ms relaxation delay, and 25 Hz line broadening with no decoupling. Frequencies were relative to trifluoroacetic acid at 0 ppm. A total of 30 000 scans per sample was acquired.

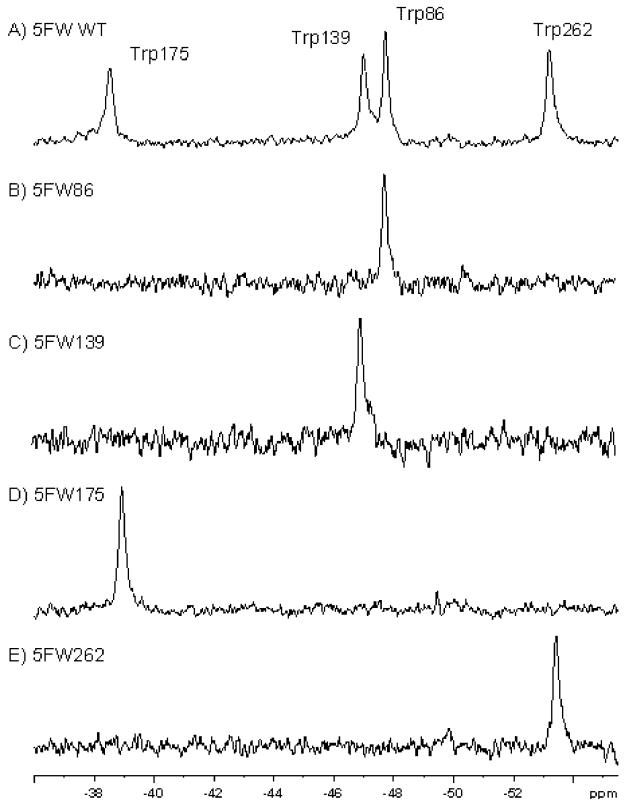

FIGURE 3: The ^{19}F NMR spectra of PAI-1s in the RCL-cleaved conformation. Proteins were cleaved between the P3−P4 residues of the RCL by fluxing 5F-Trp-labeled PAI-1s through a 1 mL NHS-activated Sepharose column coupled with elastase: (A) cleaved 5FW wt, (B) cleaved 5FW86, (C) cleaved 5FW139, (D) cleaved 5FW175, and (E) cleaved 5FW262. Protein samples and spectral measurements were the same as those described in Figure 1. A total of 40 000 scans per sample was acquired.

maintained the active form and did not revert to the latent form during the period of the experiment, we monitored the NMR sample by SDS−PAGE. Prior to and immediately after collection of the data, a 25 μL aliquot of protein from the NMR tube was added to a stoichiometric amount of t-PA and resolved on an SDS gel. Inspection of the gel revealed identical amounts of PAI-1 in complex with t-PA for both cases (data not shown). The spectrum of 5FW wtPAI-1 (Figure 2A) shows four well-resolved resonances. Assignments for each of the four resonances to specific tryptophan residues were accomplished using site-directed mutagenesis in which three of the four tryptophan residues were replaced with phenylalanine to produce the single tryptophan mutants. Subsequently, 5F-Trp was biosynthetically incorporated into these mutants using the auxotrophic system developed earlier (*47*, *48*), and the corresponding ^{19}F NMR spectra are shown in Figure 2B−E. The resonances observed in the spectra of the single tryptophan mutants permitted the assignment of each resonance observed in wt protein to a specific tryptophan residue. ^{19}F NMR were also measured for the cleaved PAI-1 mutants (Figure 3) and for PAI-1 mutants in complex with t-PA (Figure 4). The ^{19}F NMR resonance assignments for all three protein forms are summarized in Table 4.

Inspection of the spectra of the single tryptophan mutants and comparison to the wt spectrum showed that there was good agreement of the resonances between the wt and the mutant proteins. The resonances observed in the spectra of 5FW86, 5FW139, and 5FW262 were within 0.1−0.3 ppm of the resonances seen in the spectrum of 5FW wtPAI-1. A larger difference existed with 5FW175, in which the resonance for Trp175 differed by ∼0.8 ppm on comparison with the 5FW wt spectrum. This would suggest that the particular combination of mutations of the Trp86, Trp139, and Trp262 residues to phenylalanine had an impact upon the local structure as reported by the spectrum of 5FW175 (Figure 2d). The ^{19}F NMR spectrum of 5FW86 (Figure 2b) showed a broad resonance centered at −50.55 ppm. No change in peak intensity or shape was observed upon increasing the temperature from 20 to 30 °C. A resonance at −49.37 ppm was observed in the spectrum of 5FW139 (Figure 2c), but unlike the peak in the 5FW86 spectrum, it was sharp and well-defined. The ^{19}F NMR spectrum of 5FW175 (Figure 2d) displays a distinct lowfield resonance observed at −39.99 ppm. The fluorine resonance observed at −52.83 ppm in the spectrum of 5FW262 (Figure 2e) was found upfield of the other three resonances.

^{19}F NMR Spectra of 5F-Trp-Incorporated Cleaved PAI-1 Mutants and PAI-1 Mutants in Complex with t-PA. In an attempt to elucidate new details of the structural changes of PAI-1 that result upon cleavage of the RCL and its insertion into β-sheet A, and also of the interaction of PAI-1 with t-PA, ^{19}F NMR experiments were performed on the 5F-Trp-incorporated PAI-1s in the cleaved conformation and in complex with t-PA. Cleaved proteins were obtained by

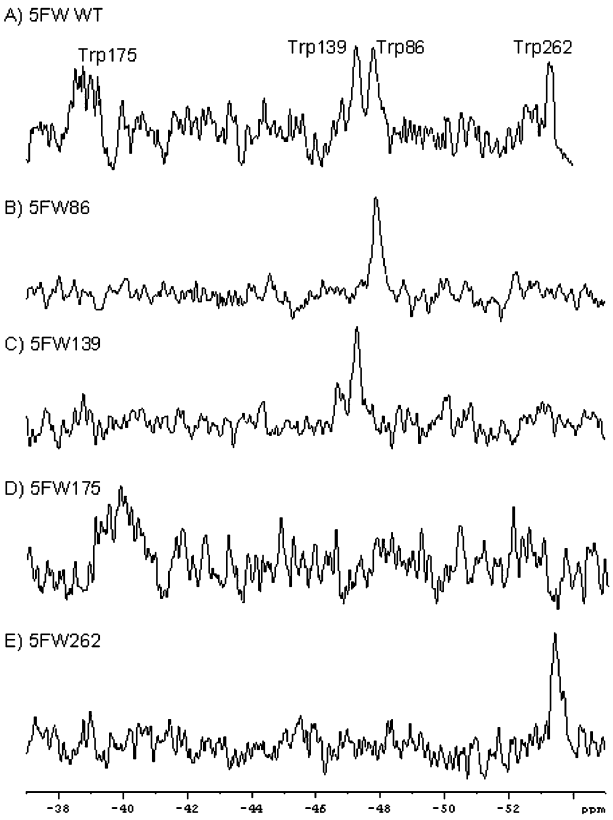

FIGURE 4: The ^{19}F NMR spectra of PAI-1s in complex with t-PA. A stoichiometric amount of t-PA in 30 mM sodium phosphate, 135 mM NaCl, 20 mM EACA, 1 mM EDTA, and pH 6.6, was added to each PAI-1 mutant: (A) 5FW wt + t-PA, (B) 5FW86 + t-PA, (C) 5FW139 + t-PA, (D) 5FW175 + t-PA, and (E) 5FW262 + t-PA. In some cases precipitation was immediately evident, while in other instances very little precipitant accumulated over the time course of the experiment. Spectral measurements were the same as those described in Figure 1 with 50 Hz line broadening. A total of 40 000 scans per sample was acquired.

Table 4: ^{19}F NMR Resonance Assignments of 5F-Trp-Labeled PAI-1s in the Active and Cleaved Forms and in Complex with t-PA[a]

	active	cleaved	complex with t-PA
5FW wt	−39.20, −49.26, −50.74, −52.57	−38.57, −46.99, −47.73, −53.20	−38.49, −47.26, −47.77, −53.35
5FW86	−50.55	−47.75	−47.87
5FW139	−49.37	−46.99	−47.33
5FW175	−39.99	−38.93	−39.07
5FW262	−52.83	−53.41	−53.44

[a] ^{19}F NMR resonance assignments (ppm) were determined from samples ranging from 50 to 80 μM in 5 mM sodium phosphate, 345 mM NaCl, 1 mM EDTA, and pH 6.6 at 20 °C. For determination of the resonance assignments of PAI-1 in complex with t-PA, t-PA in 30 mM sodium phosphate, 135 mM NaCl, 20 mM EACA, 1 mM EDTA, and pH 6.6 was added in a stoichiometric amount to PAI-1 samples and run under the same conditions as that for the active and cleaved forms as described in the Materials and Methods.

fluxing PAI-1 proteins through a 1 mL Sepharose column that had been coupled with elastase. Elastase cleaved the RCL at the P3−P4 residues, without forming a covalent complex with PAI-1, thus allowing loop insertion to occur (*60*). To ensure that cleavage was complete, a small aliquot of the column effluent was mixed with t-PA and run on a 10% SDS−PAGE with nonreducing sample buffer. The gel did not show a band corresponding to the MW of the PAI-1/t-PA complex. This observation reflected the inability of PAI-1 to form an adduct with t-PA and, in conjunction with the observed electrophoretic migration of PAI-1, was taken as confirmation of RCL cleavage (data not shown). Figure 3 shows the ^{19}F NMR spectra of the RCL cleaved proteins. On comparison of the active PAI-1 spectra, peak sharpening was seen in the spectra of cleaved 5FW86, 5FW175, and 5FW262 mutants. There was a negligible increase in the line width observed in the spectra of cleaved 5FW139. Table 5 summarizes the line widths of the four tryptophan residues in PAI-1 in both the active and cleaved forms. Significant downfield chemical shifts were observed in the spectra of the cleaved 5FW86 (∼2.8 ppm) and 5FW139 (∼2.4 ppm) and to a lesser extent in cleaved 5FW175 (∼1 ppm). A smaller upfield chemical shift (∼0.6 ppm) was observed in the cleaved 5FW262 spectrum.

Table 5: Line Widths of Assigned 5F-Trp-Labeled Residues of Active and Cleaved wtPAI-1[a]

residue	active (Hz)	cleaved (Hz)
Trp86	294	122
Trp139	141	150
Trp175	222	165
Trp262	179	147

[a] Line widths (Hz) were determined at half-height of the peak intensity. Line broadening of 25 Hz was used in processing the spectra and not subtracted from the data shown in the table.

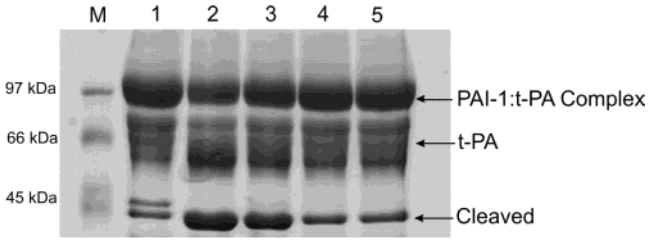

FIGURE 5: SDS−PAGE gel showing the relative amounts of cleaved and complexed 5F-Trp-labeled PAI-1 variants. Samples were removed upon completion of NMR experiments, mixed with nonreducing sample buffer, and resolved on 10% SDS−PAGE: lane 1, 5FW wt; lane 2, 5FW86; lane 3, 5FW139; lane 4, 5FW175; lane 5, 5FW262; lane M, low molecular weight markers.

^{19}F NMR spectra from experiments in which a stoichiometric amount of t-PA was added to PAI-1 variants are shown in Figure 4. Owing to the amount of precipitation in the NMR tube upon addition of t-PA to PAI-1, several attempts were required to achieve satisfactory spectra. To ensure that the spectra acquired from these experiments were indeed that of PAI-1 in complex with t-PA, a small aliquot was removed from all NMR sample tubes after data acquisition was completed. These aliquots were briefly centrifuged, and the supernatant was resolved on a nonreducing SDS−PAGE gel. These results are shown in Figure 5. Another consideration was the stability of the complex over the time course of the experiment such that breakdown of the complex (i.e., deacylation) did not occur to any significant degree. Appropriately, all PAI-1 variants were mixed with t-PA and resolved on a 10% SDS gel after a period of 15 min and 14 h following mixing. Inspection of the gels showed no change in the nature of the complex over the time frame of the NMR experiments (data not shown). The chemical shifts observed of PAI-1 variants in the complex with t-PA were almost identical to the shifts

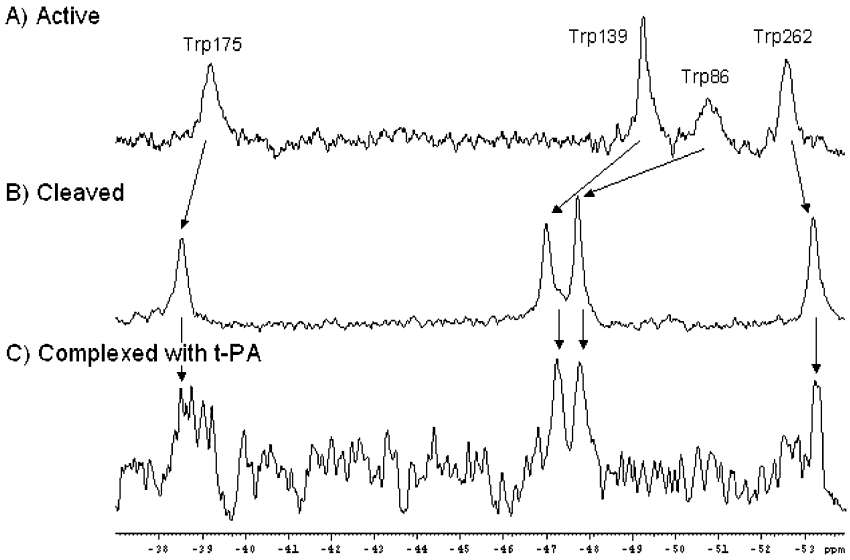

FIGURE 6: The ^{19}F NMR spectra of 5FW wtPAI-1 in the active and cleaved forms and in complex with t-PA. A comparison of the spectra of 5F-Trp-labeled wtPAI-1 demonstrating the chemical shifts and peak appearances in the (A) active conformation, (B) cleaved conformation, and (C) in complex with t-PA is shown. Protein samples and spectral measurements were the same as those described in Figure 1 with 50 Hz line broadening for the complexed spectra.

observed in the cleaved forms of PAI-1 mutants shown in Figure 3. The most notable observation was that of the spectrum of 5FW175 in complex with t-PA (Figure 4d) where the peak broadened significantly. Upon increase of the temperature of the 5FW175/t-PA complex from 20 to 30 °C, no changes were observed in the spectrum. It was not possible to measure line widths of the t-PA complexed forms owing to inadequate resolution of the peaks from the baseline. Figure 6 shows the ^{19}F NMR spectra of the 5F-Trp-labeled wild-type protein in its active, cleaved, and complexed forms, demonstrating the chemical shifts resulting from RCL cleavage and its subsequent insertion into the body of the serpin.

DISCUSSION

Efficiency of 5F-Trp Incorporation into PAI-1 and its Effect on PAI-1 Expression and Function. Various methods have been used to assess the level of tryptophan analogue incorporation in proteins (*66*, *67*). Mass spectral analysis is one method frequently used to characterize proteins (*68*) and thus may be a method to assess the level of analogue incorporation. Biosynthetic incorporation of aromatic amino acid analogues into proteins provides a useful strategy by which one can investigate structure and function relationships using fluorescence (*48*). In such work, it is necessary to determine the level of incorporation of the analogue into the protein of interest.

An alternative to determine analogue incorporation was required. Sulfonic acids are nonoxidizing strong acids and have been shown to be appropriate for protein hydrolysis leading to quantitative tryptophan determination (*63*, *69*). Such methods of analogue quantitation have been developed and were used in this work (unpublished data) (*62*). The incorporation efficiency for most mutants was satisfactory. Evidence that the fluorine moiety has an effect on PAI-1 function was suggested by a decreased k_{app} observed in 5FW wt PAI-1 on comparison to its natural tryptophan counterpart. All 5F-Trp-labeled variants displayed inhibitory activity toward t-PA, but altered kinetic properties suggest that the tryptophan to phenylalanine replacements have an effect upon the inhibitory activities of these proteins toward t-PA. This implies that slight conformational changes have occurred due to the fluorine substitution and reduction of the size of the amino acid from tryptophan to phenylalanine. In other work where tryptophan analogues have been incorporated into proteins, lower levels of expression were observed in these proteins (*70*).

^{19}F NMR Spectra of 5F-Trp-Incorporated PAI-1. NMR methods provide information on conformational changes and structural dynamics that is not available in structures obtained by X-ray crystallography. It has been shown in this work that 5F-Trp can be incorporated into PAI-1. This permitted a ^{19}F NMR study of PAI-1 in its active, cleaved, and complexed forms. The ^{19}F NMR spectra of 5FW wt in its native, cleaved, and complexed forms (Figure 6) show four distinct resonances and indicated that each tryptophan residue experiences a unique environment.

The ^{19}F NMR resonances of the three forms reveal important aspects of the changes in the local structures containing tryptophan residues that take place upon cleavage of PAI-1. There is a consistency when one compares the ^{19}F NMR resonance changes between the active and cleaved forms with those seen in the changes in the crystal structure of the same species. There are significant changes in the local structures in the vicinity of Trp86 and Trp139, while there are only small changes observed in the vicinity of Trp175 and Trp262. The importance of the observations reported herein is the high degree of similarity of the resonances for the cleaved and t-PA complexed forms. No crystal structure data exist for this latter complex. This work indicates that the structure of the t-PA complex form is similar to that of the cleaved form. The observation of extensive broadening of the resonance observed in the spectrum of 5FW175 in complex with t-PA may be due to a change in the chemical shift anisotropy. The total molecular weight of the complex being much greater than that of the cleaved form would lead to a large increase in the rotational correlation time of the complex. However, one would expect a similar line broaden-

ing to occur for the other 5F-Trp resonances in the protein. An alternate rationalization would be that the local conformational flexibility of the protein segment containing the Trp175 residue is reduced in the complex, becoming conformationally restricted, and thus a broadening of the ^{19}F resonance was observed. This report provides new information on the structure of PAI-1 in its complex with t-PA showing that segments containing Trp86, Trp139, and Trp262 are similar to that in the cleaved form while Trp175 becomes conformationally restricted.

There were additional local structural features that the resonance positions initially suggested on going from the active form to the cleaved/complexed forms. For example, the changes observed in the ^{19}F NMR spectra would indicate that Trp86 and Trp139 were deshielded and suggested a more hydrophobic environment. These inferences come from studies by Robertson et al. (*71*) in which these investigators had characterized the ^{19}F chemical shifts of 5-fluoroindole (5FI) in various environments. In their report, Robertson et al. had stated that the ^{19}F resonance of 5FI moves downfield with decreasing solvent polarity. On the basis of this work alone without crystal structure evidence, one would assume that the Trp86 and Trp139 residues become more buried upon RCL cleavage. The Trp175 resonance position was also highly unusual and was suggestive of a deeply buried residue. Again, without crystal structure information, the Trp262 resonance position would be rationalized as a highly shielded solvent-exposed environment. Close examination of the crystal structure(s) appears to be inconsistent with aspects of these interpretations. However, interactions from local structural elements seen in the crystal structure(s) may rationalize these anomalous resonance positions and add to the database for interpretation of ^{19}F NMR resonances in proteins.

Trp86 is located at the turn connecting helix D with strand 2A. The ^{19}F resonance observed in the active 5FW86 spectra at −50.55 ppm is consistent with Trp86 being in a solvent-exposed environment. The broadness of this peak was attributed to the conformational freedom of the 5F-Trp residue, where the fluorine atom is sampling a variety of structural conformers in a medium exchange regime (*50*). The fluorine on this tryptophan residue may be experiencing a segmental change that is modulated by the neighboring Pro85 residue. The cis−trans isomerization of Pro85 may contribute to the broad peak observed in both the active 5FW wt and 5FW86 spectra at this resonance position. This has been suggested before in the case of the GGR in which Pro231 is in van der Waals contact with Trp133 (*50*). RCL cleavage by either elastase or reaction with t-PA resulted in the largest downfield chemical shift of the 5FW86 resonance observed for the four tryptophan residues. This would suggest that in cleavage or complexation, Trp86 moves into a less solvent-exposed environment. There was also a dramatic sharpening of this resonance. Changes in solvent accessibility alone cannot account for the downfield chemical shift reported in the cleaved and complexed spectra. Other structural elements may explain the change in the chemical shift. Residues within a 5 Å radius of the Trp86 residue in the active conformation were observed to have significantly increased their distance from Trp86 in the cleaved form. Specifically, the oxygen atoms of the carboxylate group of Glu90 are 3.9 Å from the C5 hydrogen of the indole ring in the active form. This distance increases to 13.5 Å in the cleaved form. Similarly for His229, the distance between the N3 nitrogen of the imidazole ring and the C5 hydrogen of the indole ring is 4.4 Å, increasing to 15.5 Å in the cleaved form. The N2 nitrogen of the imidazole ring of His364 is 6.1 Å from the C5 hydrogen of the indole ring in the active form, increasing to 10.7 Å in the cleaved form. In the serpin's active form, these residues (Figure 7a) may shield the fluorine on the Trp86 residue, resulting in the higher field resonance observed than what one would expect for a typical solvent-exposed residue. The movement of these residues away from Trp86 concomitant with RCL cleavage may lead to the loss of this shielding and thus contribute to the downfield chemical shift observed in the cleaved and complexed spectra.

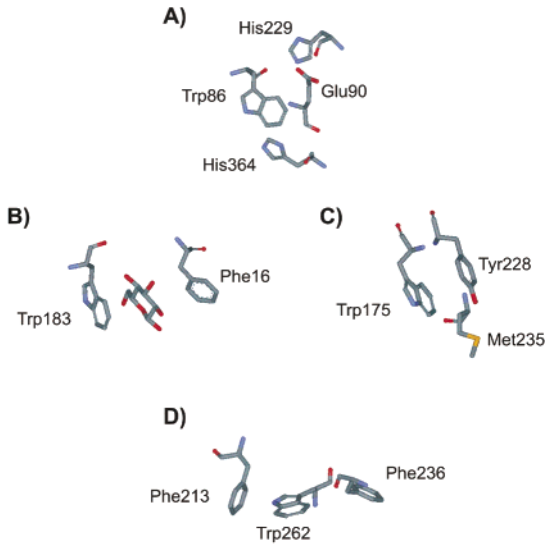

FIGURE 7: The local environment of Trp86, Trp175, and Trp262 in the active form of PAI-1 (*26*): (A) The charged residues Glu90, His229, and His364 are 3.9, 4.4, and 6.1 Å from the C5 hydrogen of the indole ring of Trp86, respectively. Examples of aromatic stacking are observed with (B) Trp183 and Phe16 of the glucose−galactose binding protein (PDB 2GBP) (*50*) and with (C) Trp175 and Tyr228 in PAI-1. The ^{19}F resonance observed for Trp183 is approximately −42.8 ppm and is within 10 Å of Phe16. D-Glucose is sandwiched between Trp183 and Phe16. The ^{19}F resonance observed for Trp175 is −39.20 ppm and is within than 4 Å from Tyr228. The aromatic rings of these two residues are coplanar. The sulfur of Met235 is within 4.6 Å from the C6 hydrogen of the indole ring of Trp175. (D) The local environment around Trp262 shows the location of residues Phe213 and Phe236 in PAI-1. All carbon atoms in the phenyl ring of Phe213 are within 3 Å from the N1 hydrogen in the indole ring of Trp262. The C1 carbon of Phe236 is within 4.6 Å from the C5 hydrogen of Trp262. Line representations follow the coloring scheme gray = carbon, blue = nitrogen, yellow = sulfur, and red = oxygen. Structures were generated in ViewerLite 5.0 (Accelrys, San Diego, CA).

Trp139 is found on the internal side of helix F, which moves during the S → R transition and facilitates β-sheet A rearrangement allowing loop insertion to occur (*5*, *11*, *72*). The chemical shift assigned to Trp139 in the active form suggests solvent exposure. The notable observation is the sharpness of this peak and is consistent with the interpretation that there is only one conformation experienced by this fluorine atom. A prominent downfield shift with a marginal increase in the peak width is shown in the cleaved 5FW139 spectrum. Inspection of the cleaved crystal structure indicates thatTrp139 becomes more buried in the protein interior. The

distance between small hydrophobic residues such as Val166 and Ala168 on s3A and the indole ring of Trp139 decreased considerably and allowed a more intimate association between these residues and Trp139. The C2 carbon of Val166 is 10.8 Å from the C5 hydrogen of Trp139 in the active form and decreases to 3.7 Å upon RCL cleavage. Likewise for Ala168, a decrease from 12.2 Å in the active form to 3.6 Å in the cleaved form between the C2 carbon and the C5 hydrogen of the indole ring are observed. This marked decrease in distance between these small aliphatic chains and the fluorine atom may account for the downfield chemical shift as the fluorine is deshielded relative to the conformation in the active form. Thus it would seem that upon RCL cleavage, the downfield shift of this resonance corresponds with an increased hydrophobic environment.

Trp175 is found at the top in the breach region connecting s3A with s3C at the point where the RCL first inserts. Trp175 is the most conserved tryptophan residue in the serpin family (*3*). The anomalous low-field assignment observed for Trp175 residue is unique in that 5F-Trp-labeled proteins rarely display a resonance this far downfield. Resonances in this spectral area have been observed in 3-fluorophenylalanine- or 4-fluorophenylalanine-labeled proteins (*50*). The 5FW175 resonance at this position could be due to the interactions of numerous aromatic residues in the near vicinity. Aromatic stacking of these residues with the fluorine could potentially shift the resonance for this fluorine to such a downfield location. Such downfield shifts, although not as dramatic, were observed with 5F-Trp183 in the GGR, in which a sugar residue was sandwiched between Trp183 and a neighboring phenylalanine and is shown in Figure 7b. (*50*). Evidence of aromatic stacking is shown in Figure 7c, in which the phenyl ring of Tyr228 is within 4 Å of the indole ring of Trp175. These two aromatic rings are almost perfectly coplanar with one another and the fluorine substituent of the Trp175 residue lies in the center of the phenyl moiety of tyrosine such that it is equidistant from all carbons of the phenyl ring. The close proximity and orientation of the two aromatic systems with respect to one another, coupled with the location of the fluorine atom may explain the particular low-field resonance observed for this residue. A large polarizable atom such as sulfur found in the nearby Met235 (Figure 7c) is within 5 Å of the C5 hydrogen on Trp175 and may also affect the shielding around Trp175. The orientation and location of all residues within a 5 Å radius of Trp175 does not change appreciably when one compares the active and cleaved conformations of PAI-1. The obvious exception is Thr333 (P14), which upon loop insertion, flips over and moves to within 5 Å of Trp175. These small structural changes may explain the small downfield chemical shift observed when loop insertion takes place. The most interesting observation as described above was that the resonance in the spectrum of 5FW175 in complex with t-PA has disappeared into the baseline (Figure 4d) while in the spectrum of the active protein a sharp peak was observed (Figure 2d).

Trp262 is located in helix H. The spectrum of active 5FW262 presented the most upfield resonance. The criteria of Robertson et al. would then suggest that this residue is the most solvent-exposed residue of the four tryptophan residues found in PAI-1. However, our fluorescence studies (unpublished data) indicate that Trp262 is the most buried residue of the four Trps in PAI-1, and this is consistent with the crystal structure (*26*, *28*). This leads us to believe that this chemical shift position in the 5FW262 spectrum is not a function of solvent exposure but a function of the local environment surrounding the fluorine atom. Danielson and Falke (*35*) have noted that van der Waals interactions may be the primary factor that influence downfield chemical shifts from that of the denatured protein resonance. The fact that resonances are also observed upfield in the denatured protein spectra would indicate some other phenomena may be responsible for these upfield shifts, and they have been attributed to electrostatic interactions (*73*, *74*). There are several suggestions for the possible origin of this anomalous chemical shift in 5FW262. Inspection of the crystal structure showed that Trp262 of helix H points inward toward β sheet B. The residues Phe213 and Phe236 of s1B and s3B, respectively, and Leu359 and Val361 of s4B form a "hydrophobic cup" around Trp262. All carbon atoms in the phenyl ring of Phe213 are less than 3 Å from the N1 hydrogen in the indole ring of Trp262. The phenyl ring of Phe213 is perpendicular to the indole ring. The C1 carbon of Phe236 is less than 4.6 Å from the C5 hydrogen of Trp262 and lies at an oblique angle to the indole ring. The magnetic effects of ring currents from these two phenylalanine residues (Figure 7d) may explain the anomalously high upfield resonance observed for 5FW262. Small upfield chemical shifts were observed in the cleaved and complexed 5FW262 spectra as a result of minor shifts in the side chains of neighboring amino acid residues. Like that of Trp175, the crystal structures of the active and cleaved forms show that the orientation and location of residues around Trp262 does not change appreciably, reflected by the small change in the chemical shift.

The cleaved and complexed spectra of 5FW86, 5FW139, and 5FW262 are quite similar, suggestive of equivalent chemical environments in both the cleaved and complexed forms. This is not surprising in the light of other studies (*13*, *18*, *20*). Stratikos and Gettins (*18*) observed that a cysteine variant of α_1-proteinase inhibitor (α_1-PI) Pittsburgh, fluorescently labeled at residue 159 of helix F, was insensitive to complex formation and concluded that the proteinase was not in contact with the external face of helix F. This is also in agreement with the crystal structure of the trypsin/α_1-antitrypsin complex (*13*). An earlier 2D NMR study of α_1-PI also indicated that there was a close correspondence in the [^{1}H$-^{15}$N] resonance positions in the spectra of the trypsin/α_1-PI complex and the cleaved α_1-PI (*20*).

It is possible that the ^{19}F spectrum of the complexed form is a composite of the cleaved and complexed species. However, the SDS gel (Figure 5) shows there is only a very small amount of cleaved 5FW wtPAI-1 in solution with 5FW wtPAI-1 in complex with t-PA (lane 1) being the dominant component. Therefore, the resonances observed in the spectrum of 5FW wtPAI-1 in complex with t-PA (Figure 4a) can be attributed to the complexed form owing to the small quantity of cleaved serpin. Similarly, the same can be said of 5FW175 and 5FW262. In the case with 5FW86 and 5FW139, there is a larger amount of the cleaved serpin in solution with the complex. However, these resonances agree well with those observed in the 5FW wtPAI-1 spectra, confirming that the cleaved and complexed forms have similar spectra. Other structural studies using proteolysis (*75*)

and fluorescence (*76*, *77*) have compared both the cleaved and complexed serpins. These studies demonstrated a very close similarity for the cleaved and complexed forms. Our data are consistent with these studies and thus support the hypothesis proposed by Wright and Scarsdale (*78*).

Last, it would be appropriate to comment on ^{19}F NMR studies of another serpin, antithrombin (AT), labeled with 6F-Trp (*49*). Like PAI-1, AT contains four tryptophan residues, three of which are conserved in PAI-1. Trp189, Trp225, and Trp307 in AT correspond to Trp139, Trp175, and Trp262 in PAI-1, respectively. Trp48 of AT and Trp86 of PAI-1 are located in different domains of their respective proteins. It is difficult to compare the relative positions of the resonances observed in these two proteins owing to the different 5F-Trp analogue used. However, it is useful to make some qualitative comparisons between the spectra of these two proteins. The authors speculate that the two overlapping resonances at −44.4 ppm belong to Trp189 and Trp225 suggesting similar buried environments. In the active 5FW wt spectrum of PAI-1 (Figure 2A) resonance assignments for Trp139 and Trp175, the analogous residues to Trp189 and Trp225 in AT, are well resolved from one another. However, the resonance assigned to a buried Trp225 at −44.4 ppm in AT makes the resonance observed at −39.99 ppm for Trp175 in PAI-1 even more remarkable, demonstrating the unique structural environment around Trp175. It would appear that the resonance assigned to Trp307 is comparable to Trp262 in PAI-1, except in the case of Trp307, a number of charged and polar residues, notably several glutamate residues, are in close proximity to Trp307 and thus the resonance observed for Trp307 is justified. This is not the case with Trp262 in which the local environment is hydrophobic with no polar residues within 8 Å. As we have suggested, the resonance for Trp262 is anomalously high owing to the proximity and orientation of hydrophobic residues as observed in the crystal structure (Figure 7d). Additional ^{19}F NMR studies on AT and PAI-1 may provide new information on the effect that local structural elements have on ^{19}F chemical shifts.

Conclusion. This report has provided additional information on structural changes that occur in PAI-1 in the active, cleaved, and complexed forms. The data show that upon RCL cleavage and loop insertion into the body of the serpin, resonances assigned to Trp86 and Trp139 undergo large downfield chemical shifts, and the data are consistent with the major structural changes observed in the crystal structures of active and cleaved PAI-1. Smaller chemical shifts were observed with Trp175 and Trp262, and these are consistent with minor structural changes observed the local environment of these residues as seen in the crystal structures. Unique ^{19}F NMR resonance assignments for 5F-Trp incorporated PAI-1s were observed for the 5FW175 and 5FW262 mutants and were attributed to local structural elements. The anomalous resonances observed for 5FW175 and 5FW262 mutants suggests that additional studies of model systems are required to understand these resonances.

ACKNOWLEDGMENT

The authors thank Jan Venne and Joe Gaspar for excellent technical support with the NMR experiments. We also thank Dr. Masoud Jelokhani-Niaraki for helpful discussions.

REFERENCES

1. Potempa, J., Korzus, E., and Travis, J. (1994) The Serpin Superfamily of Proteinase Inhibitors: Structure, Function, and Regulation, *J. Biol. Chem. 269*, 15957−15960.
2. Gils, A., and Declerck, P. J. (1998) Structure−Function Relationships in Serpins: Current Concepts and Controversies, *Thromb. Haemostasis 80*, 531−541.
3. Irving, J. A., Pike, R. N., Lesk, A. M., and Whisstock, J. C. (2000) Phylogeny of the Serpin Superfamily: Implications of Patterns of Amino Acid Conservation for Structure and Function, *Genome Res. 10*, 1845−1864.
4. Silverman, G. A., Bird, P. I., Carrell, R. W., Church, F. C., Coughlin, P. B., Gettins, P. G. W., Irving, J. A., Lomas, D. A., Luke, C. J., Moyer, R. W., Pemberton, P. A., Remold-O′Donnell, E., Salvesan, G. S., Travis, J., and Whisstock, J. C. (2001) The Serpins Are an Expanding Superfamily of Structurally Similar but Functionally Diverse Proteins, *J. Biol. Chem. 276*, 33293−33296.
5. Gettins, P. G. W. (2002) Serpin Structure, Mechanism, and Function, *Chem. Rev. 102*, 4751−4803.
6. Schick, C., Pemberton, P. A., Shi, G. P., Kamachi, Y., Cataltepe, S., Bartuski, A. J., Gornstein, E. R., Bromme, D., Chapman, H. A., and Silverman, G. A. (1998) Cross-Class Inhibition of the Cysteine Proteinases Cathepsins K, L, and S by the Serpin Squamous Cell Carcinoma Antigen 1: A Kinetic Analysis, *Biochemistry 37*, 5258−5266.
7. Irving, J. A., Steenbakkers, P. J., Lesk, A. M., Op den Camp, H. J., Pike, R. N, and Whisstock, J. C. (2002) Serpins in Prokaryotes, *Mol. Biol. Evol. 19*, 1881−1890.
8. Huber, R., and Carrell, R. W. (1989) Implications of the Three-Dimensional Structure of α_1-Antitrypsin for Structure and Function of Serpins, *Biochemistry 28*, 8951−8966.
9. Schechter, I., and Berger, A. (1967) On the size of the active site in proteases. I. Papain, *Biochem. Biophys. Res. Commun. 27*, 157−162.
10. Loebermann, H., Tokuoka, R., Deisenhofer, J., and Huber, R. (1984) Human alpha 1-proteinase inhibitor. Crystal structure analysis of two crystal modifications, molecular model and preliminary analysis of the implications for function, *J. Mol. Biol. 177*, 531−557.
11. Whisstock, J. C., Skinner, R., Carrell, R. W, and Lesk, A. M. (2000) Conformational Changes in Serpins: I. The Native and Cleaved Conformations of α_1-Antitrypsin, *J. Mol. Biol. 295*, 651−665.
12. Lawrence, D. A., Ginsburg, D., Day, D. E., Berkenpas, M. B., Verhamme, I. M., Kvassman, J.-O., and Shore, J. D. (1995) Serpin-Protease Complexes Are Trapped as Stable Acyl-Enzyme Intermediates, *J. Biol. Chem. 270*, 25309−25312.
13. Huntington, J. A., Read, R. J., and Carrell, R. W. (2000) Structure of a serpin-protease complex shows inhibition by deformation, *Nature 407*, 923−926.
14. Engh, R. A., Huber, R., Bode, W., and Schulze, A. J. (1995) Divining the serpin inhibition mechanism: a suicide substrate 'springe', *Trends Biotechnol. 13*, 503−510.
15. Lawrence, D. A., Olson, S. T., Palaniappan, S., and Ginsburg, D. (1994) Serpin Reactive Center Loop Mobility Is Required for Inhibitor Function but Not for Enzyme Recognition, *J. Biol. Chem. 269*, 27657−27662.
16. Stratikos, E., and Gettins, P. G. W. (1997) Major proteinase movement upon stable serpin-proteinase complex formation, *Proc. Natl. Acad. Sci. U.S.A. 94*, 453−458.
17. Plotnick, M. I., Mayne, L., Schechter, N. M., and Rubin, H. (1996) Distortion of the Active Site of Chymotrypsin Complexed with a Serpin, *Biochemistry 35*, 7586−7590.
18. Stratikos, E., and Gettins, P. G. W. (1998) Mapping the Serpin-Proteinase Complex Using Single Cysteine Variants of α_1-Proteinase Inhibitor Pittsburgh, *J. Biol. Chem. 273*, 15582−15589.
19. Stratikos, E., and Gettins, P. G. W. (1999) Formation of the covalent serpin-proteinase complex involves translocation of the proteinase by more than 70 Å and full insertion of the reactive center loop into β-sheet A, *Proc. Natl. Acad. Sci. U.S.A. 96*, 4808−4813.
20. Peterson, F. C., and Gettins, P. G. W. (2001) Insight into the Mechanism of Serpin-Proteinase Inhibition from 2D [^{1}H-^{15}N] NMR Studies of the 69 kDa α_1-Proteinase Inhibitor Pittsburgh−Trypsin Covalent Complex, *Biochemistry 40*, 6284−6292.
21. Ginsburg, D., Zehab, R., Yang, A. Y., Rafferty, U. M., Andreasen, P. A., Nielsen, L., Dano, K., Lebo, R. V., and Gelehrter, T. D.

(1986) cDNA Cloning of Human Plasminogen Activator-Inhibitor from Endothelial Cells, *J. Clin. Invest. 78*, 1673−1680.
22. van Mourik, J. A., Lawrence, D. A., and Loskutoff, D. J. (1984) Purification of an Inhibitor of Plasminogen Activator (Antiactivator) Synthesized by Endothelial Cells, *J. Biol. Chem. 259*, 14914−14921.
23. Kruithof, E. K. O., Tran-Thang, C., Ransijn, F., and Bachmann, F. (1984) Demonstration of a fast-acting inhibitor of plasminogen activators in human plasma, *Blood 64*, 907−913.
24. Blouse, G. E., Perron, M. J., Thompson, J. H., Day, D. E., Link, C. A., and Shore, J. D. (2002) A Concerted Structural Transition in the Plasminogen Activator-1 Mechanism of Inhibition, *Biochemistry 41*, 11997−12009.
25. Mottonen, J., Strand, A., Symersky, J., Sweet, R. M., Danley, D. E., Geoghegan, K. F., Gerard, R. D., and Goldsmith, E. J. (1992) Structural basis for latency in plasminogen activator inhibitor-1, *Nature 355*, 270−273.
26. Sharp, A. M., Stein, P. E., Pannu, N. S., Carrell, R. W., Berkenpas, M. B., Ginsburg, D., Lawrence, D. A., and Read, R. J. (1999) The active conformation of plasminogen activator inhibitor 1, a target for drugs to control fibrinolysis and cell adhesion, *Struct. Fold. Des. 7*, 111−118.
27. Nar, H., Bauer, M., Stassen, J.-M., Lang, D., Gils, A., and Declerck, P. J. (2000) Plasminogen Activator Inhibitor 1. Structure of the Native Serpin, Comparison to its Other Conformers and Implications for Serpin Inactivation, *J. Mol. Biol. 297*, 683−695.
28. Aertgeerts, K., DeBondt, H. L., De Ranter, C. J., and Declerck, P. J. (1995) Mechanisms contributing to the conformational and functional flexibility of plasminogen activator inhibitor-1, *Nat. Struct. Biol. 2*, 891−897.
29. Boström, S., Deinum, J., Löfroth, J.-E, Wirth, M., and Kubista, M. (1990) Conformational Differences between Latent and Active Plasminogen Activator Inhibitor, PAI-1: A Spectroscopic Study, *Thromb. Res. 59*, 851−858.
30. Dwivedi, A. M., Woodeshick, R. W., Walton, H. L., and Reilly, T. M. (1991) A Spectroscopic Study of the Conformations of Active and Latent Forms of Recombinant Plasminogen Activator Inhibitor-1, *Biochem. Biophys. Res. Commun. 175*, 437−443.
31. Seetharam, R., Dwivedi, A. M., Duke, J. L., Hayman, A. C., Walton, H. L., Huckins, N. R., Kamerkar, S. M., Corman, J. I., Woodeshick, R. W., Wilk, R. R., and Reilly, T. M. (1992) Purification and Characterization of Active and Latent Forms of Recombinant Plasminogen Activator Inhibitor 1 Produced in *Escherichia coli*, *Biochemistry 31*, 9877−9882.
32. Lawrence, D. A., Olson, S. T., Palaniappan, S., and Ginsburg, D. (1994) Engineering Plasminogen Activator Inhibitor 1 Mutants with Increased Functional Stability, *Biochemistry 33*, 3643−3648.
33. Sancho, E., Declerck, P. J., Price, N. C., Kelly, S. M., and Booth, N. A. (1995) Conformational Studies on Plasminogen Activator Inhibitor (PAI-1) in Active, Latent, Substrate, and Cleaved Forms, *Biochemistry 34*, 1064−1069.
34. Schulze, A. J., Quarzago, D., and Andreasen, P. A. (1996) A spectroscopic study of the structures of latent, active and reactive-center-cleaved type-1 plasminogen-activator inhibitor, *Eur. J. Biochem. 240*, 550−555.
35. Danielson, M. A., and Falke, J. J. (1996) Use of ^{19}F NMR to Probe Protein Structure and Conformational Changes, *Annu. Rev. Biophys. Biomol. Struct. 25*, 163−195.
36. Gerig, J. T (1994) Fluorine NMR of Proteins, *Prog. Nucl. Magn. Reson. Spectrosc. 26*, 293−370.
37. Wüthrich, K. (1986) *NMR of Proteins and Nucleic Acids*, Wiley, New York.
38. Gettins, P. (1987) Antithrombin III and Its Interaction with Heparin. Comparison of the Human, Bovine, and Porcine Proteins by ^{1}H NMR Spectroscopy, *Biochemistry 26*, 1391−1398.
39. Gettins, P., and Harten, B. (1988) Properties of Thrombin- and Elastase-Modified Human Antithrombin III, *Biochemistry 27*, 3634−3639.
40. Hood, D. B., and Gettins, P. (1991) A ^{1}H NMR Probe for Mobility in the Reactive Center Loops of Serpins: Spin−Echo Studies of Native and Modified Forms of Ovalbumin and α_1-Proteinase Inhibitor, *Biochemistry 30*, 9054−9060.
41. Matheson, N. R., van Halbeek, H., and Travis, J. (1991) Evidence for a Tetrahedral Intermediate Complex during Serpin-Proteinase Interactions, *J. Biol. Chem. 266*, 13489−13491.
42. Horne, A., and Gettins, P. (1992) ^{1}H NMR Spectroscopic Studies on the Interactions between Human Plasma Antithrombin III and Defined Low Molecular Weight Heparin Fragments, *Biochemistry 31*, 2286−2294.
43. Perkins, S. J., Smith, K. F., Nealis, A. S., Haris, P. I., Chapman, D., Bauer, C. J., and Harrison, R. A. (1992) Secondary structure changes stabilize the reactive-centre cleaved forms of SERPINS. A study by ^{1}H nuclear magnetic resonance and Fourier transform infrared spectroscopy, *J. Mol. Biol. 228*, 1235−1254.
44. Peterson, F. C., Gordon, N. C., and Gettins, P. G. W. (2000) Formation of a Noncovalent Serpin-Proteinase Complex Involves No Conformational Change in the Serpin. Use of ^{1}H-^{15}N HSQC NMR as a Sensitive Nonperturbing Monitor of Conformation, *Biochemistry 39*, 11884−11892.
45. Pervushin, K., Riek, R., Wider, G., and Wüthrich, K. (1997) Attenuated T2 relaxation by mutual cancellation of dipole−dipole coupling and chemical shift anisotropy indicates an avenue to NMR structures of very large biological macromolecules in solution, *Proc. Natl. Acad. Sci. U.S.A. 94*, 12366−12371.
46. Salzmann, M., Pervushin, K., Wider, G., Senn, H., and Wüthrich, K. (1998) TROSY in triple-resonance experiments: new perspectives for sequential NMR assignment of large proteins, *Proc. Natl. Acad. Sci. U.S.A. 95*, 13585−13590.
47. Hogue, C. W. V., Rasquinha, I., Szabo, A. G., and McManus, J. P. (1992) A new intrinsic fluorescent probe for proteins. Biosynthetic incorporation of 5-hydroxytryptophan into oncomodulin, *FEBS Lett. 310*, 269−272.
48. Ross, J. B. A, Szabo, A. G., and Hogue, C. W. V. (1997) Enhancement of Protein Spectra with Tryptophan Analogues: Fluorescence Spectroscopy of Protein-Protein and Protein-Nucleic Acid interactions, *Methods Enzymol. 278*, 151−190.
49. Gettins, P., Choay, J., Crews, B. C., and Zettlmeiss, G. (1992) Role of Tryptophan 49 in the Heparin Cofactor Activity of Human Antithrombin III, *J. Biol. Chem. 267*, 21946−21953.
50. Luck, L. A., and Falke, J. J. (1991) ^{19}F NMR Studies of the D-Galactose Chemosensory Receptor. 1. Sugar Binding Yields a Global Structural Change, *Biochemistry 30*, 4248−4256.
51. Salopek-Sondi, B., and Luck, L. A. (2002) ^{19}F NMR study of the leucine-specific binding protein of *Escherichia coli*: mutagenesis and assignment of the 5-fluorotryptophan-labeled residues, *Protein Eng. 15*, 855−859.
52. Kunkel, T. A., Roberts, J. D., and Zakour, R. A. (1987) Rapid and efficient site-specific mutagenesis without phenotypic selection, *Methods Enzymol. 154*, 367−382.
53. Kunkel, T. A., Bebenek, K., and McClary, J. (1991) Efficient site-directed mutagenesis using uracil-containing DNA, *Methods Enzymol. 204*, 125−139.
54. Blouse, G. E., Perron, M. J., Kvassman, J.-O., Yunus, S., Thompson, J. H., Betts, R. L., Lutter, L. C., and Shore, J. D. (2003) Mutation of the highly conserved tryptophan in the serpin breach region alters the inhibitory mechanism of Plasminogen Activator Inhibitor-1, *Biochemistry 42*, 12260−12272.
55. Olson, S. T., Bock, P. E., Kvassman, J.-O., Shore, J. D., Lawrence, D. A., Ginsburg, D., and Bjork, I. (1995) Role of the catalytic serine in the interactions of serine proteinases with protein inhibitors of the serpin family. Contribution of a covalent interaction to the binding energy of serpin-proteinase complexes, *J. Biol. Chem. 270*, 30007−30017.
56. Sambrook, J. E., Fritsch, E. F., and Maniatis, T. (1989) *Molecular Cloning: A Laboratory Manual*, Cold Spring Harbor Laboratory, Cold Spring Harbor, NY.
57. Bradford, M. M. (1976) A rapid and sensitive method for the quantitation of microgram quantities of protein utilizing the principle of protein-dye binding assays, *Anal. Biochem. 72*, 248−254.
58. Kvassman, J.-O., and Shore, J. D. (1995) Purification of Human Plasminogen Activator Inhibitor (PAI-1) from *Escherichia coli* and Separation of its Active and Latent Forms by Hydrophobic Interaction Chromatography, *Fibrinolysis 9*, 215−221.
59. Vaughan, D. E., Declerck, P. J., Reilly, T. M., Park, K., Collen, D., and Fasman, G. D. (1993) Dynamic structural and functional relationships in recombinant plasminogen activator inhibitor-1, *Biochim. Biophys. Acta 1202*, 221−229.
60. Wu, K., Urano, T., Ihara, H., Takada, Y., Fujie, M., Shikimori, M., Hashimoto, K., and Takada, A. (1995) The cleavage and inactivation of plasminogen activator inhibitor type 1 by neutrophil elastase: the evaluation of its physiologic relevance in fibrinolysis, *Blood 86*, 1056−1061.
61. Kvassman, J.-O., Verhamme, I., and Shore, J. D. (1998) Inhibitory Mechanism of Serpins: Loop Insertion Forces Acylation of Plasminogen Activator by Plasminogen Activator Inhibitor-1, *Biochemistry 37*, 15491−15502.

62. Abbott, G. L. (2003) Quantitation of Tryptophan Analogues Biosynthetically Incorporated into Proteins and Structural Investigation of Single Tryptophan Mutants of Plasminogen Activator Inhibitor-1, M. Sc. Thesis, University of Waterloo, Waterloo, ON, Canada.
63. Penke, B., Ferenczi, R., and Kovacs, K. (1974) A New Acid Hydrolysis Method for Determining Tryptophan in Peptides and Proteins, *Anal. Biochem. 60*, 45−60.
64. Delhaye, S., and Landry, J. (1986) High Performance Liquid Chromatography and Ultraviolet Spectrophotometry for Quantitation of Tryptophan in Barytic Hydrolysates, *Anal. Biochem. 159*, 175−178.
65. Tian, W. X., and Tsou, C. L. (1982) Determination of the rate constant of enzyme modification by measuring the substrate reaction in the presence of the modifier, *Biochemistry 21*, 1028−1032.
66. Waxman, E., Rusinova, E., Hasselbacher, C. A., Schwartz, G. P., Laws, W. R., and Ross, J. B. A. (1993) Determination of the tryptophan:tyrosine ratio in proteins, *Anal. Biochem. 210*, 425−428.
67. Senear, D. F., Mendelson, R. A., Stone, D. B., Luck, L. A., Rusinova, E., and Ross, J. B. A. (2002) Quantitative Analysis of Tryptophan Analogue Incorporation in Recombinant Proteins, *Anal. Biochem. 300*, 77−86.
68. Siuzdak, G. (1996) *Mass Spectrometry for Biotechnology*, Academic Press, San Diego, CA.
69. Simpson, R. J., Neuberger, M. R., and Liu, T.-Y. (1976) Complete amino acid analysis of proteins from a single hydrolysate, *J. Biol. Chem. 251*, 1936−1940.
70. Hasselbacher, C. A., Rusinova, R., Rusinova, E., and Ross, J. B. A. (1995) in *Techniques in Protein Chemistry* (Crabb, J. W., Ed.) Vol. 6, pp 349−356, Academic Press, New York.
71. Robertson, D. E., Kroon, P. A., and Ho, C. (1977) Nuclear magnetic resonance and fluorescence studies of substrate-induced conformational changes of histidine-binding protein J of *Salmonella typhimurium*, *Biochemistry 16*, 1443−1451.
72. Vleugels, N., Gils, A., Bijnens, A.-P., Knockaert, I., and Declerck, P. J. (2000) The importance of helix F in plasminogen activator inhibitor-1, *Biochim. Biophys. Acta 1476*, 20−26.
73. de Dios, A. C., Pearson, J. G., and Oldfield, E. (1993) Secondary and tertiary structural effects on protein NMR chemical shifts: an ab initio approach, *Science 260*, 1491−1496.
74. Pearson, J. G., Oldfield, E., Lee, F. S., and Warshel, A. (1993) Chemical shifts in proteins: a shielding trajectory analysis of the fluorine nuclear magnetic resonance spectrum of the *Escherichia coli* galactose binding protein using a multipole shielding polarizability-local reaction field-molecular dynamics approach, *J. Am. Chem. Soc. 115*, 6851−6862.
75. Egelund, R., Schousboe, S. L., Sottrup-Jensen, L., Rodenburg, K. W., and Andreasen, P. A. (1997) Type-1 plasminogen-activator inhibitor: conformational differences between latent, active, reactive-centre-cleaved and plasminogen-activator-complexed forms, as probed by proteolytic susceptibility, *Eur. J. Biochem. 248*, 775−785.
76. Fa, M., Bergstrom, F., Hagglof, P., Wilczynska, M., Johansson, L. B.-A., and Ny, T. (2000) The structure of a serpin-protease complex revealed by intramolecular distance measurements using donor-donor energy migration and mapping of interaction sites, *Struct. Fold. Des. 8*, 397−405.
77. Fa, M., Bergstrom, F., Karolin, J., Johansson, L. B.-A., and Ny, T. (2000) Conformational studies of plasminogen activator inhibitor type 1 by fluorescence spectroscopy. Analysis of the reactive centre of inhibitory and substrate forms, and of their respective reactive-centre cleaved forms, *Eur. J. Biochem. 267*, 3729−3734.
78. Wright, H. T., and Scarsdale, J. N. (1995) Structural basis for serpin inhibitor activity, *Proteins 22*, 210−225.

BI035618A